

The memory kernel of the self-intermediate scattering function on a MD-simulated glass-forming $\text{Ni}_{20}\text{Zr}_{80}$ -system

A.B. Mutiara

Graduate Program In Information System,
Gunadarma University,

Jln. Margonda Raya 100, Depok 16424, Indonesian.

(Dated: July 31, 2008)

The memory kernel of the self-part of the intermediate scattering function is studied. We found that the short-time behavior of the memory kernel for our MD-simulated glass-forming $\text{Ni}_{20}\text{Zr}_{80}$ -system shows a deviation from the polynomial form predicted by MCT. By using the gaussian approximation we give a more detailed description of the short-time dynamics of the system.

PACS numbers:

I. INTRODUCTION

At present the phenomena behind the liquid-glass transition and the nature of the glassy state are not fully understood, despite the progresses of recent years. In contrast to usual phase transformations the glass transition seems to be primarily dynamic in origin and therefore new theoretical approaches have to be developed for its description. Several theoretical models have been proposed to explain the transition and the corresponding experimental data. The latter concern of both *the temperature dependence of particular properties*, such as the shear viscosity and the structural relaxation time, and *the time dependence response of the spectra* as visible in the dielectric susceptibility, inelastic neutron scattering, and light scattering spectra investigations. The spectral measurements have been extended to cover the large frequency range from below the primary α -relaxation peak up to the high-frequency region of microscopic dynamics dominated by vibrational modes [1].

One of the promising approaches in this field is mode coupling theory (MCT). MCT originally was developed to model critical phenomena [2, 3]. The non-classical behavior of the transport properties near the critical point was thought to be caused by nonlinear couplings between slow (hydrodynamics and order parameter) modes of the system. In later years, the MCT was found to be applicable more generally, to describe nonlinear effects in dense liquids [4] and nonhydrodynamic effects in the case of the glass transition.

The idealized schematic model of the MCT for the liquid-glass transition, firstly proposed by Bengtzelius et.al. [5] and independently by Leutheusser [6], implies that the liquid ("ergodic") state is characterized through a decay of structural correlations while below a critical temperature T_c a solidlike ("nonergodic") state exists with structural arrest where fluctuations are effectively frozen. In this state correlations decay on a longer time scale by thermally activated diffusion processes [7, 8, 9].

According to the MCT the time dependence of the correlation functions for structural fluctuations follows from a damped harmonic oscillator equation with a retarded

damping term. All the details concerning the time evolution of the structural correlations are hidden in the memory kernel that describes the retarded damping.

In a previous paper [10], hereafter referred to as I, one of us has evaluated this memory kernel from the time dependence of the correlation functions in the molecular dynamics(MD) simulations of the glass-forming $\text{Ni}_{50}\text{Zr}_{50}$ -system. Here two results from I shall be recalled: first, it found that the short-time behavior of the memory kernel of the self-part of the intermediate scattering function $\Phi(q, t)$ shows a deviation from the polynomial form commonly assumed in the idealized(or extended) schematic model of the MCT. This deviation, in particular, explains the absence of the inverse powerlaw decay of the correlation predicted by the MCT. The deviations originate from the vibrational motions of the atoms in local potential minima and are restricted to the short times, below some 0.3 ps. This, on the other hand, explains that the MCT predictions for the late β -regime and for the α -peak are in a good agreement with the experimental results [11, 12, 13, 14, 15] and MD-simulation [16, 17]. Second, there is a characteristic quantity g_m , as introduced in [18], that can be used as a relative measure to describe how close a liquid structure has approached the arrested nonergodic state. If $g_m > 1$ for a given temperature T , then the system is able to undergo the transition into an idealized nonergodic state with a structural arrest; if $g_m < 1$, the system remains in the (undercooled) liquid state ($T > T_c$), and if $g_m \approx 1$, the system stands in a critical situation.

The behavior of the memory kernel $F(t)$ and the parameter g_m are formally related through the characteristic function $g(\Phi) = F(t)/(1/\Phi(q, t) - 1)$ introduced in [18]. g_m means the maximum of $g(\Phi)$ for $\Phi \in [0, 1]$ and the short time behavior of $F(t)$ is, in particular, visible in the behavior of $g(\Phi)$ for values $\Phi(q, t) \rightarrow 1$. Therefore we here are interested in a detailed description of $g(\Phi)$ for short times, respectively $\Phi(q, t) \rightarrow 1$. Since, according to I, $\Phi(q, t)$ for short times is determined by the vibration spectrum of the amorphous structure, the memory kernel $F(t)$ for short times and the corresponding g also depend on the vibration spectrum. The latter is visible in the velocity autocorrelation function (VACF) and

thus we in the following look for an interrelationship between the VACF and g . Moreover, we here consider the $\text{Ni}_{1-x}\text{Zr}_x$ system at $x = 0.8$, while in I the concentration $x = 0.5$ was investigated. Thus we ask to which extend the results for $x = 0.8$ confirm the results for $x = 0.5$ from I.

Our paper is organized as follows: In Section II, we present the model and give some details of the computations. Section III gives a brief discussion of some aspects of the mode coupling theory as used here and it describes the gaussian approximation to relate $\Phi(q, t)$ and the VACF at the short time. Results of our MD-simulations and their analysis are then presented and discussed in Section IV.

II. SIMULATIONS

As in paper I, the present simulations are carried out as state-of-the-art isothermal-isobaric (N, T, p) calculations. The Newtonian equations of $N = 648$ atoms (130 Ni and 518 Zr) are numerically integrated by a fifth order predictor-corrector algorithm with time step $\Delta t = 2.5 \times 10^{-15}$ s in a cubic volume with periodic boundary conditions and variable box length L . With regard to the electron theoretical description of the interatomic potentials in transition metal alloys by Hausleitner and Hafner [19] we model the interatomic couplings as in [20] by a volume dependent electron-gas term $E_{vol}(V)$ and pair potentials $\phi(r)$ adapted to the equilibrium distance, depth, width, and zero of the Hausleitner-Hafner potentials [19] for $\text{Ni}_{20}\text{Zr}_{80}$ [21]. For this model simulations were started through heating a starting configuration up to 2000 K, yielding a homogeneous liquid state. The system then is cooled continuously to various annealing temperatures with cooling rate $-\partial T = 1.5 \times 10^{12}$ K/s. Afterwards the obtained configurations of various annealing temperatures (here 1500-800 K) are relaxed by modelling an additional isothermal annealing that depend on the object temperature. Finally the time evolution of these relaxed configurations is modelled and analyzed. Full details of the simulations are given in [21].

III. THEORY

A. Mode Coupling Theory

In the MCT equation of motion for the correlation function of structural fluctuations with wave vector \mathbf{q} can be expressed as a damped harmonic oscillator equation (see, e.g., [22, 23])

$$\ddot{\Phi}(q, t)/\Omega_0^2 + \Phi(q, t) + \int_0^t d\tau F(q, t - \tau)\dot{\Phi}(q, \tau) = 0 \quad (1)$$

with initial conditions $\Phi(q, 0) = 1$ and $\dot{\Phi}(q, 0) = 0$. Ω_0 is a microscopic (phonon) frequency and $F(t)$ is the memory kernel. The schematic model assumes that the time

dependence of $F(q, t)$ can be expressed by that of $\Phi_q(t)$ and the idealized version of MCT, neglecting atomic diffusion, relies on the assumption

$$F(q, t) = F_0(t) := h(t) + f(\Phi(q, t)) \quad (2)$$

where $f(\Phi)$ means the polynomial in Φ and $h(t)$ a short time viscous damping which conveniently is approximated by an instantaneous term $\eta_0\delta(t)$. The asymptotic behavior of $\Phi(q, t)$ is determined by $f(\Phi)$.

As mentioned above, there is for a given temperature a characteristic function $g(\Phi)$ whose maximum value can be used to determine whether the system is able to undergo a structural arrest ($g_m > 1$) or whether it remains in the (undercooled) liquid state ($g_m < 1$). This characteristic function can be derived as follows: Given $\lim_{t \rightarrow \infty} \Phi \approx \Phi^\infty > 0$. Let us assume that there is a critical time t_c so that for $t > t_c$

$$\dot{\Phi}(t) = 0, \quad (3)$$

$$\ddot{\Phi}(t) = 0. \quad (4)$$

Substitute the equations (3) and (4) in MCT-Eq. (1), then the MCT-Eq. becomes

$$\Phi^\infty + f(\Phi^\infty)(\Phi^\infty - 1) = 0, \quad (5)$$

and after a little algebra we find

$$g(\Phi) = f(\Phi)(1/\Phi - 1) \quad (6)$$

with $\Phi \in [0, 1]$. This function is related in simple way to $\Delta F(\Phi) = f(\Phi) - \Phi/(1 - \Phi)$ frequently used in the schematic MCT [24].

According to the extended version of MCT which simulates atomic diffusion by taking into account the coupling to transverse currents, the memory kernel has the following form

$$F(t) = \mathcal{L}^{-1}\{1/[D(z) + \frac{1}{\mathcal{L}(F_0(t))_z}]\} \quad (7)$$

Here \mathcal{L} means the Laplace transform, \mathcal{L}^{-1} its inverse. $D(z)$ models the coupling to the transverse currents. $F(t)$ from Eq.(7) leads to the final decay of structural fluctuations also below T_c . This sets one of the basic problems in classification of the solutions of Eq.(1) as it may not be obvious for a given solution whether it belongs to the regime above or below T_c if atomic diffusion is included.

For our analysis we introduce the Laplace Transform for the memory kernel $F(t)$ and the correlation function $\Phi(t)$, by taking $z = \varepsilon - i\omega$ with $\varepsilon \rightarrow 0$, as follows

$$\lim_{\varepsilon \rightarrow 0} \mathcal{L}\{F(t)\}_{\varepsilon - i\omega} = F_c(\omega) + iF_s(\omega) \quad (8)$$

$$\lim_{\varepsilon \rightarrow 0} \mathcal{L}\{\Phi(t)\}_{\varepsilon - i\omega} = \Phi_c(\omega) + i\Phi_s(\omega) \quad (9)$$

where $\Phi_c(\omega)$ and $\Phi_s(\omega)$ are the cosines-part and sinus-part of the Fourier transformed $\Phi(t)$. It should be noted

that according to the fluctuation-dissipation theorem the loss part of the dynamic susceptibility spectrum $\chi''(\omega)$ is related to the dynamics structure factor $\Phi_c(\omega)$ via

$$\chi''(\omega) = \omega \Phi_c(\omega) \quad (10)$$

Substitute equations (8) and (9) in MCT-Eq. (1), then we obtain the equation for the spectral distribution $\omega F_c(\omega)$ of the memory kernel

$$\omega F_c(\omega) = \frac{\omega \Phi_c(\omega)}{[1 - \omega \Phi_s(\omega)]^2 + [\omega \Phi_c(\omega)]^2}. \quad (11)$$

Taking the inverse-Fourier transformed $F_c(\omega)$, we have the time dependent memory kernel

$$F(t) = \frac{2}{\pi} \int_0^\infty d\omega F_c(\omega) \cos(\omega t). \quad (12)$$

B. Gaussian Approximation

According to the theoretical models studied in the theory of liquids [25, 26, 27] we want to illustrate the correlation functions in the short-time regime for temperatures near the critical temperature. One of the models based on a cumulant expansion [28] express the correlation function in an isotropic system

$$\Phi(q, t) = \exp \{-q^2 \rho_1(t) + q^4 \rho_2(t) - \dots\}, \quad (13)$$

where

$$\rho_1(t) = \frac{1}{6} \langle |\mathbf{x}_i(t+t_0) - \mathbf{x}_i(t_0)|^2 \rangle, \quad (14)$$

$$\rho_2(t) = \frac{1}{2} [\rho_1(t)]^2 [R_2(t) - 1], \quad (15)$$

$$R_2(t) = \frac{3}{5} \frac{\langle |\mathbf{x}_i(t+t_0) - \mathbf{x}_i(t_0)|^4 \rangle}{\left[\langle |\mathbf{x}_i(t+t_0) - \mathbf{x}_i(t_0)|^2 \rangle \right]^2} \quad (16)$$

The assumption that $\Phi(q, t)$ can be expressed only by the leading term of expansion [25, 28]

$$\Phi(q, t) = \exp \left\{ -\frac{q^2}{6} \langle |\mathbf{r}(t+t_0) - \mathbf{r}(t_0)|^2 \rangle \right\} \quad (17)$$

is called the Gaussian approximation. Also in this approximation the correlation function is related to one-sixth the mean square displacement (MSD) of atoms during time t . In section IV. we will show our calculating results of Eq.(17) and prove that this approximation is correct in the short-time regime.

To show, by using this Gaussian approximation, whether our system in the short-time regime is a purely harmonic system or not, we need a relation between the mean squared displacement and the spectral distribution $Z(\omega)$ of the velocity autocorrelation function $Z(t)$ and a

assumption that in purely harmonic system $Z(\omega)$ would be proportional to the density of state (DOS) $Z_{dos}(\omega)$. One find that relation

$$\langle |\mathbf{r}(t+t_0) - \mathbf{r}(t_0)|^2 \rangle = 6\omega_0^2 \int_0^\infty d\omega \frac{(1 - \cos(\omega t))}{\omega^2} Z(\omega), \quad (18)$$

where

$$\begin{aligned} Z(\omega) &= \int_0^\infty dt \cos(\omega t) Z(t) \\ &= \int_0^\infty dt \cos(\omega t) \frac{\langle v_i(t+t_0) \cdot v_i(t_0) \rangle}{\langle |v_i(t_0)|^2 \rangle}, \end{aligned} \quad (19)$$

$$\omega_0^2 = \frac{1}{3} \langle |v_i(t_0)|^2 \rangle = \frac{k_B T}{M} \quad (20)$$

Actually Ngai et.al.(see e.g. [29]) have developed a model, which is called "Coupling-Model", in order to explain the dynamics of glass-forming liquids. Here we briefly review that model. The model made use of the assumption that vibration (phonon) and relaxation (diffusion) of the molecules contribute independently to the density-density correlation function; thus, $\Phi(q, t)$ is equal to the product $\Phi_{ph}(q, t) \times \Phi_{relax}(q, t)$ [30]. In this model the correlation function of the relaxation $\Phi_{relax}(q, t)$

$$\Phi_{relax}(q, t) = \begin{cases} \exp(-t/t_0(q, T)) & \text{for } t < t_c \\ \exp(-(t/\tau(q, T))^{1-n}) & \text{for } t > t_c \end{cases}, \quad (21)$$

where respectively t_c is a temperature-independent crossover time separating two time regimes in which the relaxation dynamics differ, t_0 the Debye-relaxation time, τ the Kohlrausch-relaxation time, and $1 - n = \beta$ the Kohlrausch stretching exponent

The phonon contribution to $\Phi(q, t)$ is determined by the harmonic DOS of the phonon modes, $Z_{dos}^{harm}(\omega)$, according to the formula (see e.g.[30, 31]), in a classical limit,

$$\Phi_{ph}(q, t) = \exp\left(-\frac{q^2}{2} u(t, T)\right), \quad (22)$$

where

$$u(t, T) = \frac{2k_B T}{M} \int_0^\infty d\omega \frac{(1 - \cos(\omega t))}{\omega^2} Z_{dos}^{harm}(\omega). \quad (23)$$

$u(t, T)$ decreases with time, leveling off to constant value $u(T) = \lim_{t \rightarrow \infty} u(t, T)$. Correspondingly, $\Phi(q, t)$ has the value $\exp(-q^2 u(T)/2)$, which is the well known Lamb-Mössbauer factor. For a single Einstein oscillator of frequency ω_e the harmonic DOS of the phonon modes is given by

$$Z_{dos}^{harm}(\omega) = \delta(\omega - \omega_e) \quad (24)$$

and, for a Debye model of a solid,

$$Z_{dos}^{harm}(\omega) = \begin{cases} 3\omega^2/\omega_D^3 & \text{for } \omega < \omega_D \\ 0 & \text{for } \omega > \omega_D \end{cases} \quad (25)$$

By comparing this expressions of the coupling model with those of the theory of liquids and making a assumption that $Z_{dos}^{harm}(\omega)$ and $Z_{dos}(\omega)$ are the same quantities in the short-time regime we find that $\Phi_{ph}(q, t)$ (Eq.(22) with Eq.(23)) of the coupling model is the same as $\Phi(q, t)$ (Eq.(17) with Eq.(18)) of the theory of liquids (with the Gaussian approximation).

Considering that the model of the theory of liquid has a simple form we use for our further analysis that model. We believe that by making use of the model it is enough to prove whether in the short-time regime our system is a harmonic system or not.

Following Cummins et.al.[1] the correlation functions $\Phi(t)$ and the corresponding susceptibility spectrum $\chi''(\omega)$ can be considered to consist of three regimes: 1) at high frequencies (short times) a nearly temperature-independent microscopic structure; 2) at low frequencies (long times) a strongly temperature-dependent α -relaxation peak associated with structural relaxation and diffusion process; 3) (intermediate frequencies) between a) and b) a minimum in $\chi''(\omega)$ (or "plateau") in $\Phi(t)$ whose amplitude and position is also temperature dependent.

From above definition of regions we write now in general form the full susceptibility spectrum

$$\chi''(T, \omega) = \chi''_{st}(T, \omega) + \chi''_{it}(T, \omega) + \chi''_{lt}(T, \omega) \quad (26)$$

After our intensive study about the short-time regime for the object temperatures near the critical temperature it is a little difficult to separate purely the short time regime from the intermediate regime. Also it is important to keep in mind that our definition for the short-time part in Eq.(26) include a small part of the β -relaxation process.

Considering that the spectral distribution of the velocity autocorrelation function $Z(t)$ for each temperature near T_c (from [19] $T_c = 1050 \pm 25K$) shows too in our system a nearly temperature-independent form (see Fig. 1), we can scale now the short-time part of the susceptibility spectrum, so that

$$\chi''_{sc}(T, \omega) = \frac{T}{T_0} \chi''_M(\omega), \quad (27)$$

where χ''_M is the master curve of the susceptibility spectrum that is now a temperature-independent quantity and is defined

$$\chi''_M(\omega) = \frac{1}{N} \sum_i^N \frac{T_0}{T_i} \chi''_{st}(T, \omega), \quad (28)$$

where N is the number of the object temperature and T_0 is a arbitrary normalization of temperature.

IV. RESULTS AND DISCUSSION

The central object of our analysis is the self-part of the intermediate scattering function:

$$\Phi(\mathbf{q}, t) = \langle \exp \{ i \mathbf{q} \cdot [\mathbf{x}_i(t + t_0) - \mathbf{x}_i(t_0)] \} \rangle. \quad (29)$$

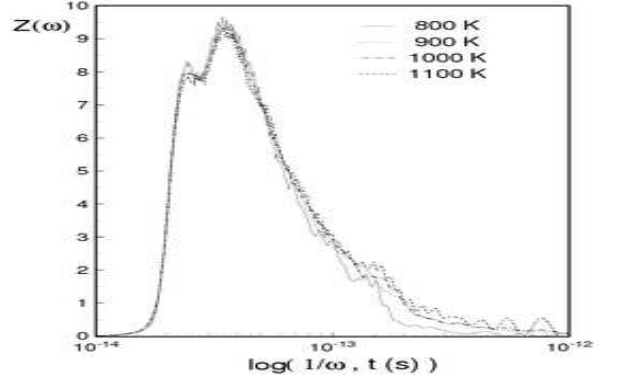


FIG. 1: The spectral distribution of the velocity autocorrelation function for different temperature near T_c .

The bracket means averages over the atom i and the initial configurations t_0 .

In Figs. 2 and 3 we show the results evaluated from our MD data (with symbols) for wave vector $q = \frac{2\pi}{L}(n, 0, 0)$ with $n = 8$ and 6 which correspond respectively to $|q| = 19.7 \text{ nm}^{-1}$ and $|q| = 14.7 \text{ nm}^{-1}$. Both figures present the average over the star of six q vectors which are equivalent on assuming equivalence of the simulation cube axis and their inverses.

A. MCT-Analysis

The following Fig. 2 and 3 present the self-part of the intermediate scattering function for different object temperatures according to MCT (with line) and our MD-simulation (with symbols). The discrepancy between both results are considerable as results from the bad fitting of the Kohlrausch-law to our MD-data and the inaccuracy by calculation (see [10, 18, 21] for details of the algorithm used for calculation).

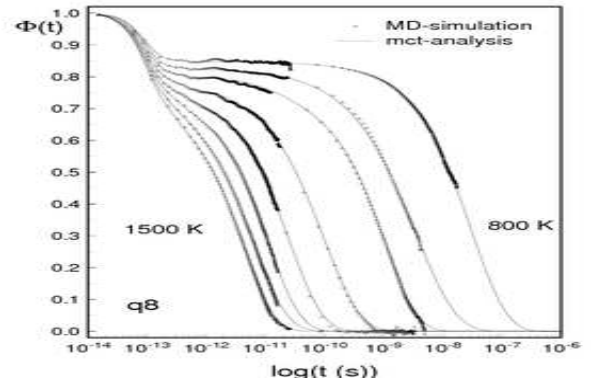


FIG. 2: The self-part of the intermediate scattering function for wave vector q_8 from MD-data (with symbol) and from MCT-Equations (with line).

From both figures we found that the self-part of the intermediate scattering function show for q_8 and q_6 at aver-

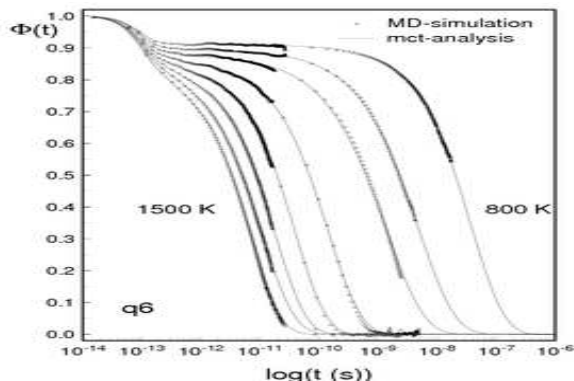


FIG. 3: The same as Fig. 2 but for q_6 .

age temperatures the structural relaxations that happen in three successive steps. According to predictions of the idealized schematic model of MCT the correlator should decay in three successive steps [20] at this temperatures. The first is a fast initial decay on the time scale of vibrations of atoms ($t < 1$ ps). This step is characterized by MCT only global. The second is the β -relaxation regime (typically in the range $1 \text{ ps} < t < 1 \text{ ns}$). In the early β -relaxation regime the correlator should decrease according to $\Phi(t) = f_c + A/t^a$ and in the late β -relaxation regime, which appear only in melting, according to von Schweidler-law $f_c - Bt^b$. Between them the wide plateau appear near the critical temperature T_c . In the case of idealized glass the von Schweidler-law does not appear more, but $\Phi(t) = f_c + A/t^a$ flows into the constant asymptotic value f_c . In melting the α -relaxation appear as the last step that results from the decay after the von Schweidler-law and could be described by the Kohlrausch-law $\Phi(t) = A_0 \exp(-(t/\tau_0)^\beta)$ whose the relaxation time τ_0 near the glass transition shifts dramatic to the longer time scale.

The decay for the early β -regime, which according to MCT follows the inverse power-law $\Phi \sim f_c + A/t^a$, could not be observed in our data. The reason for it is that in our system $\Phi_m(T)$ (the maximum of $g(\Phi)$) and $\Phi_o(T)$ (the threshold-value of $G(\Phi)$, see Eq.(33)) are nearly parallel, which cause that the power-law of the early β -regime is dressed up. On the one side, for this regime the so-called “Boson-peak” is discussed by several authors (see e.g.[32, 33, 34]), on the other side one called this peak as the β -maximum [35]. The first group of authors claimed that as a result of the atomic vibrations in the β -regime the boson-peak in a glass-system is observed, which depends on the fragility of the system. The more fragile the system is, the weaker is the effects of the atomic vibrations, i.e., the height of a boson-peak will be observed smaller and not clearer. As a result the relaxation-process is here observed clearer. In a connection with the fragility the glass-systems can be classified into two groups [32, 36]: 1) fragile glass-systems, which have no directional bonds, e.g., Van der Waals and ionic systems. These glass formers exhibit

strong non-Arrhenius-like increase of the viscosity upon cooling; 2) strong glass-systems, which have strong directional bonds. These glass-systems have the temperature dependence of the viscosity that is more Arrhenius like and weaker.

In a connection with this classification it is until today still difficult to determine whether the metallic-glass belongs to a strong glass-system or to a fragile glass-system, because usually the behavior of the viscosity in a metallic glass-system lies between both borderline case. So far from in hand analysis of our data we can state nothing about the “Boson-peak”.

We observed that the self-part of the intermediate scattering function for $T < T_c$ shows a small bump at $t \approx 2.5 \times 10^{-12} \text{ s}$. The same phenomenon was observed on MD-simulations for a OTP-system by Lewis and Wahnström [17] and for a binary Lennard-Jones mixture by Kob and Andersen [16]. This bump is interpreted by those authors as a result of the finite-size effect. The same bump was also observed on another Lennard-Jones mixture-system [37], on a liquid-salt system [38], and on a colloidal-suspension system [39].

We have also analyzed that the height of plateaus as well as the time scale, at which the self-part of the intermediate scattering function decay finally to zero, depend strongly on wave vector q . Our MD-results of $\Phi(q, t)$ for the longer time show that $\Phi(q, t)$ always decay to zero at both $T < T_c$ and $T > T_c$. We interpret this result within the scope of the extended schematic MCT. The extended schematic MCT predicts that the long-time behavior of $\Phi(q, t)$ always decay to zero, when thermally activated hopping-processes is taken to be account in a system. According to Teichler [10, 18, 40] and Aspelmeier [41] these hopping-processes take place on a MD-simulated $\text{Ni}_{50}\text{Zr}_{50}$. As one can there observe, the reason for decays of $\Phi(q, t)$ on the longer time scale is that on this time scale thermally activated hopping-processes run off. To prove this statement, we have to investigate the self-diffusion constant of atoms in our atoms. The MCT predicts that self-diffusion constant follows a power-law that is a function of T_c :

$$D_\alpha \propto (T - T_c)^\gamma \quad (30)$$

where $\gamma = 1/(2a) + 1/(2b)$ is valid and by knowing of the exponent λ can be calculated. α is the specific atom. The estimation of γ over that expression is only possible, if a q -independence exponent λ is given as required by deriving that expression. On MD-simulation we can determine for different temperatures of interest the self-diffusion constant through the calculation of mean squared displacement (MSD). Then we find the curve D_α vs T . The effective exponent γ can be determined by using the least-squared method. From the curve we can prove whether the thermally activated hopping-processes run off at $T < T_c$ or temperatures near T_c in our system or not, as we investigate whether there is a deviation from (30) or not. If there is this deviation, then it means that the hopping processes still take place at

$T < T_c$ or T near T_c [40, 42].

From above discussion we can state that the behavior of $\Phi(q, t)$ in our system agree with the prediction of the extended MCT, in which the long-time behavior of $\Phi(q, t)$ decays to zero as a result of the atomic diffusion.

The MCT predicts that the behavior of $\Phi(q, t)$ in the last α -regime can be good approximated by the Kohlrausch-law. We have determined the Kohlrausch's parameters A_0 , β , and τ_0 . Our results show that the parameter in our system (see Table I) depends weakly on wave vectors q and varies with temperature. The β -value increases with a decreasing q -value about 0.05. This result is similar as one by Lewis and Wahnström in MD-simulated OTP-system [17].

On our results we have noticed that the β -value seem to increase to one at higher temperatures with a decreasing q -value. This phenomane is also found in another MD-simulation by Bernu et.al. [43]. The MCT predicts that β -value for $q \sim q_0$ ($\sim 20 \text{ nm}^{-1}$), which corresponds to a nearest-neighbor distance, is found typically in range $0.6 < \beta < 0.8$ that depends on the system of interest; for $q \ll q_0$ the β -value seem to increase. Also our β -value agrees well with the MCT's predictions.

According to MCT the α -relaxation time diverge near T_c after the power-law [42, 44]

$$\tau_0(T) \propto (T - T_c)^\gamma \quad (31)$$

where γ is the same exponent in Eq.(30). On our results we have found that the behavior of the power-law was broken in the nearest environments from T_c , because as a result of thermally activated atomic diffusion the α -relaxation time τ_0 kept to a finite-value.

Through a viewing of the α -relaxation time τ_0 we have found that this relaxation time has a strong depending on q -value. The same result was observed in a MD-simulated binary Lenard-Jones mixture by Kob and Andersen [16] and in a experimental quasy-elastic neutron scattering on three polymers by Colmenero et.al. [45]. We have noticed that there is an anomaly on the α -relaxation time, namely, the relaxation time increases drastic near the glass-transition. One explains this anomaly [46]: the system is found above T_c on the way to a metastable equilibrium of undercooled liquid-phases. Then the system comes below T_c into a unstable state, where the relaxation processes take place in a direction of the equilibrium. On grounds of this anomaly we can state that the glass transition actually is a dynamic transition which is more in the change of the art on atomic movements and less in the change of the structure [41, 47]

Figures 4 and 5 present the dynamic susceptibility. From both figures we found that there are three different frequency-regimes of the dynamics susceptibility as mentioned in theory section. As predicted by extended MCT the α -peak shift with a decreasing temperature to the lower frequency, und this peak and the minimum of the dynamics susceptibility are no more dissapear at temperature near T_c . The extended MCT assumes this behavior, when thermally activited hopping-processes are included

TABLE I: The Kohlrausch parameters A_0 , τ_0 , β fitted to $\Phi(q, t)$ from MD-data for wave vector q_8 and q_6 .

T [K]	$q_8 = 19.7 \text{ [nm}^{-1}\text{]}$			$q_6 = 14.7 \text{ [nm}^{-1}\text{]}$		
	A_0	τ_0 [ns]	β	A_0	τ_0 [ns]	β
1500	0.690	0.004	0.807	0.821	0.007	0.917
1400	0.729	0.007	0.820	0.827	0.011	0.821
1300	0.746	0.012	0.840	0.835	0.018	0.911
1200	0.759	0.024	0.780	0.859	0.042	0.781
1100	0.761	0.095	0.740	0.860	0.146	0.795
1000	0.790	0.966	0.748	0.859	~ 1.400	0.813
900	0.826	~ 2.448	0.680	0.894	~ 4.871	0.741
800	0.848	~ 31.100	0.756	0.911	~ 38.640	0.794

formally in the memory kernel $F(t)$. These processes has taken place in our system, i.e., these predictions agree with statements mentioned above.

We have noticed that the height of α -peak for each temperature depends strongly on q -value, namely, the height of α -peak decreases with a increasing q -value. The microscopic (phonon)-regime as well as the height of this regime decreases with a decreasing both q -value and T . This result could be simply interpreted, if one takes into consideration the height of plateaus (the non-ergodicity parameter f_c) on the intermediate scattering function, which depends strongly on the q -value. Because the height of the α -peak is proportional to the height of plateaus, and the microscopic-peak is proportional to $1 - f_c$, then the above mentioned dependence of the both height-peaks results directly from the q -dependence non-ergodicity paramater.

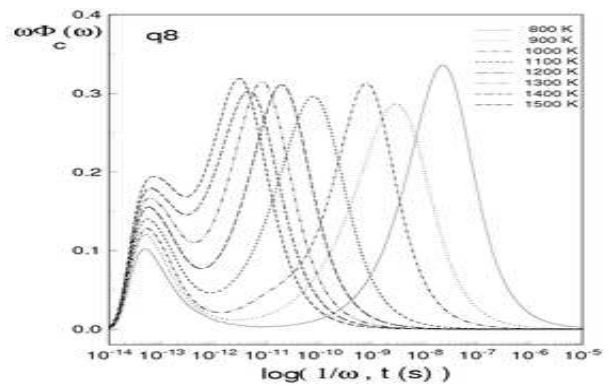


FIG. 4: The dynamic susceptibility for wave vector q_8

Figures 6 and 7 present our evaluated kernels $F(t)$ from MD-data of $\Phi(q, t)$ for both wave vectors of interest. From both figures we found that there is a temperature-dependence threshold-value $\Phi_0(T)$ ($\Phi_0(T) \in [0; 1]$), where under $\Phi_0(T)$ the behavior of $F(t)$ shows a course that corresponds to a polynomial with positive coefficients, and otherwise this behavior deviates from a polynomial form. According to the prediction of the idealized MCT

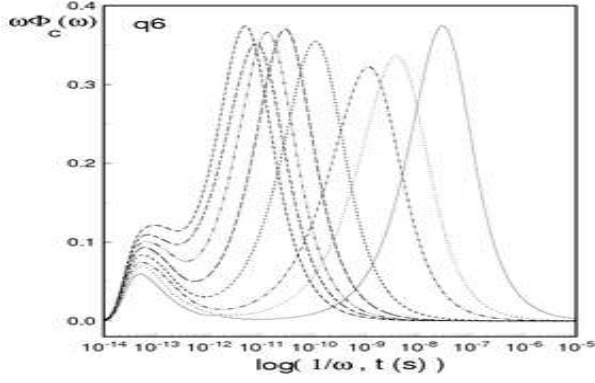


FIG. 5: The same as Fig. 4, but for wave vector q_6

the kernel $F(t)$ as well as $f(\Phi)$ should show a polynomial form. Also our results do not agree with this prediction for all of regimes, but only for the regime that lies under $\Phi_0(T)$. This is understandable, because the idealized MCT does not fully describe the atomic vibrations of the system.

We have noticed that $\Phi_0(T)$ depends strongly on the q -value and weakly on the change of temperature. $\Phi_0(T)$ shift with a decreasing both q -value and T to higher values.

There is here a important point that we can stretch, namely, by a calculating of the kernel $F(t)$ we can make for $\Phi(T) < \Phi_0(T)$ a new model of the memory kernel $f(\Phi)$, which presents of course a polynomial form. By a extending for $\Phi(T) > \Phi_0(T)$ we can then determine the term, which could be assigned to the atomic vibrations of the system and corresponds to the difference between the actually kernel $F(t)$ and the fitted memory kernel $f(\Phi)$. To this purpose we present our calculating for the kernel $F(t)$ as a function Φ in Fig. 8 and 9. According to MCT one define $f(\Phi)$ as follows :

$$f(\Phi) = \sum_n \lambda_n \Phi^n \quad (32)$$

where λ_n are positive coefficients. We have fitted Eq.(32) to the kernel $F(\Phi)$. (see Fig. 10 and 11), and then we have for our system positive coefficients λ_n , which are given in Tables II and III

To calculate Eq.(6), as in I, we introduce the following equations

$$G(\Phi) := F(\Phi)(1/\Phi - 1) \quad (33)$$

$$g(\Phi) = P(\Phi)(1/\Phi - 1) \quad (34)$$

Eq.(34) is analog to Eq.(6), where $f(\Phi)$ in $g(\Phi)$ is substituted by $P(\Phi)$. When we have calculated for $\Phi(T) < \Phi_0(T)$ $F(\Phi)$ as well as $f(\Phi)$, i.e., in compliance with both equations we also have calculated for $\Phi(T) < \Phi_0(T)$ the function $P(\Phi)$. Therefore we can now state that $P(\Phi)$ is also a polynomial function with positive coefficients

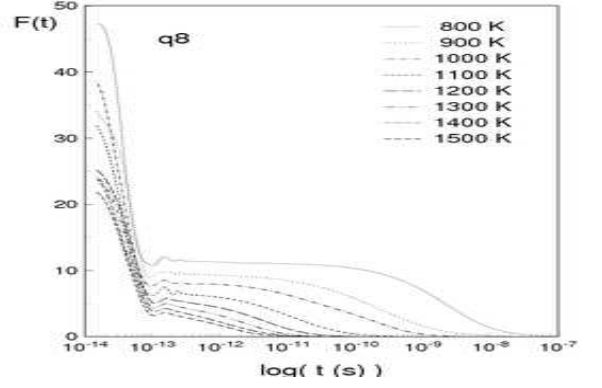


FIG. 6: The kernel $F(t)$ for wave vector q_8 .

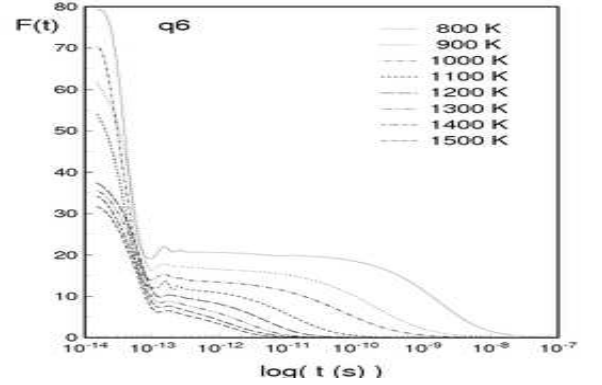


FIG. 7: The same as Fig. 6 but for wave vector q_6 .

λ_n , which will fit for $\Phi(T) < \Phi_0(T)$ the function $g(\Phi)$ to $G(\Phi)$.

In Figs. 12 and 13 we present the $G(\Phi)$ -function. From both figures we can see that $G(\Phi)$ has a maximum at $\Phi_0(T)$. This maximum shifts with a decreasing q -value to a higher value. We can now fit the function $g(\Phi)$, which contains the polynomial function $P(\Phi)$ with positive coefficients (see Tables. II and III), to $G(\Phi)$. Our results is shown in Figs. 14 and 15. From both figures we have for each temperature a maximum g_m from $g(\Phi)$ -

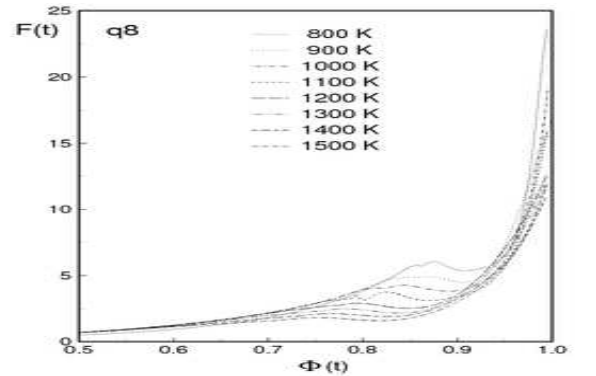
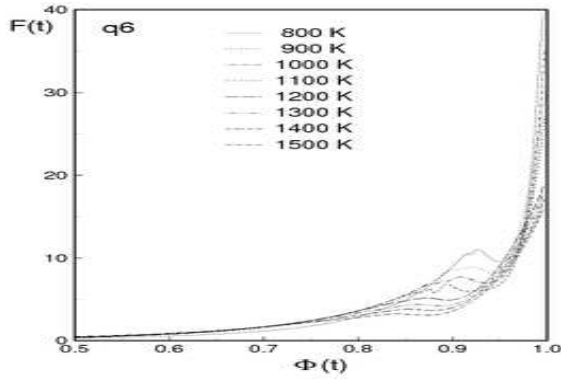
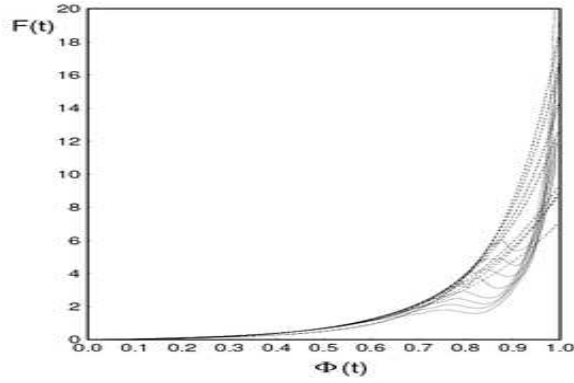
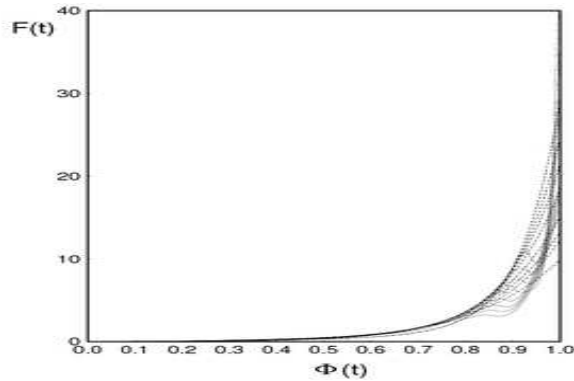


FIG. 8: The kernel as a function of Φ for wave vector q_8 .

FIG. 9: The same as Fig. 8 but for wave vector q_6 .FIG. 10: The kernel as function of Φ for wave vector q_8 (dotted line: extrapolated low- Φ polynomial).

function at $\Phi = \Phi_m$. This maximum is smaller als 1 for $T \geq 1100$ K ($g_m < 1$), and for $T \leq 1000$ K nearly equal 1 ($g_m \approx 1$).

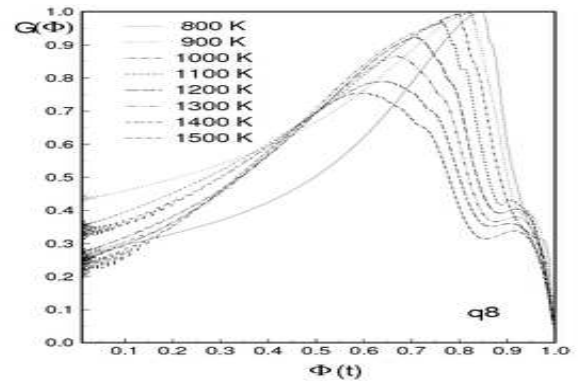
As mentioned in the theory section, g_m describes a signature, so that, if $g_m < 1$, the system is in a ergodic state (in a liquid state), and if $g_m > 1$, it is in a non-ergodic state (in a structural arrest). Our results show that the $\text{Ni}_{20}\text{Zr}_{80}$ -system is for $T \geq 1100$ K in a liquid state and for $T \leq 1000$ K nearly in a structural arrest

FIG. 11: The same as Fig. 10 but for wave vector q_6 .TABLE II: Coefficients of the polynomial expansion $f(\Phi) = \sum_n \lambda_n \Phi^n$ for wave vector q_8 .

		λ_n							
		T K							
n		800	900	1000	1100	1200	1300	1400	1500
1		0.255	0.423	0.232	0.357	0.271	0.253	0.308	0.198
2		0.714	0.794	0.658	0.688	0.661	0.598	0.820	0.800
3		0.040	0.597	1.757	1.177	1.174	1.630	1.165	1.592
4		1.390	1.318	2.144	1.621	2.089	1.850	1.876	2.628
5		2.218	1.930	1.637	1.655	2.535	2.116	1.439	0.057
6		1.586	1.628	0.700	1.817	2.414	1.828	0.593	1.769
7		0.321	0.621	0.000	1.445	0.232	0.566	0.742	0.040
8		0.000	0.000	0.009	1.251	0.012	0.000	2.089	0.185
9		2.438	1.575	1.552	0.623	0.032	0.000	0.002	0.143
10		9.864	8.069	5.907	2.253	0.040	0.020	0.000	0.451

TABLE III: Coefficients of the polynomial expansion $f(\Phi) = \sum_n \lambda_n \Phi^n$ for wave vector q_6 .

		λ_n							
		T K							
n		800	900	1000	1100	1200	1300	1400	1500
1		0.235	0.316	0.362	0.246	0.173	0.189	0.240	0.162
2		0.021	0.386	0.373	0.246	0.394	0.278	0.394	0.135
3		0.918	0.924	0.990	0.965	0.214	0.612	0.682	0.515
4		1.291	0.994	1.240	1.006	0.529	0.810	0.640	1.397
5		0.016	0.588	0.873	0.127	1.448	1.323	1.563	2.250
6		0.102	0.130	0.289	0.009	2.594	2.528	2.250	4.494
7		0.001	0.000	0.000	1.780	3.493	2.873	2.756	0.689
8		0.000	0.249	0.366	4.877	3.671	4.101	1.277	0.185
9		0.001	1.238	1.893	6.649	2.645	0.563	1.166	0.063
10		0.000	3.152	5.013	2.365	0.020	0.003	0.003	0.001
11		3.192	7.167	10.157	0.092	0.030	0.303	1.323	0.003
12		8.222	7.978	0.002	0.044	0.042	0.005	0.001	0.014
13		15.148	1.400	0.000	0.013	0.011	0.002	0.002	0.000

FIG. 12: $G(\Phi)$ for wave vector q_8 according to Eq.(33).

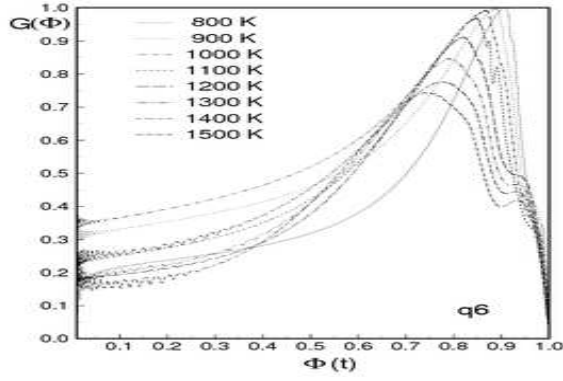


FIG. 13: The same as Fig. 12 but for wave vector q_6 .

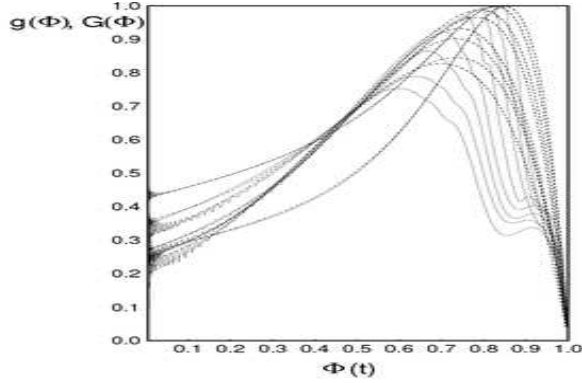


FIG. 14: Fitting $g(\Phi)$ (dotted lines) to $G(\Phi)$ (full lines) for wave vector q_8 according to Eqs.(34) and (33).

with a correlation decay, which is as a result of a thermally activated atomic diffusion. In Fig. 16 we present a curve g_m vs T for each q -value. From that Fig. one can see that our system has a critical temperature T_c between 1000 K and 1100 K. Here we decide T_c as about

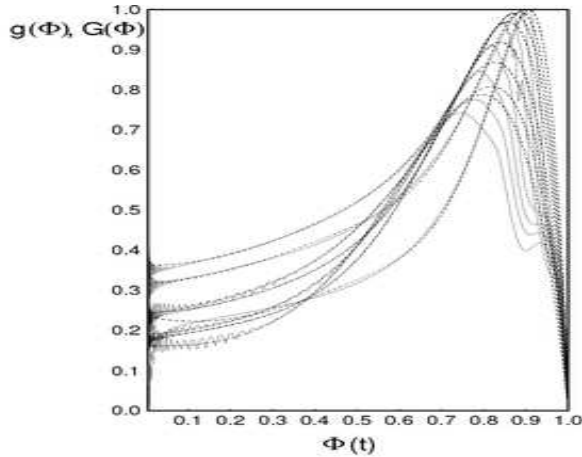


FIG. 15: Fitting $g(\Phi)$ (dotted line) to $G(\Phi)$ (full lines) for wave vector q_6 according to Eqs.(34) and (33).

(1025 ± 25) K.

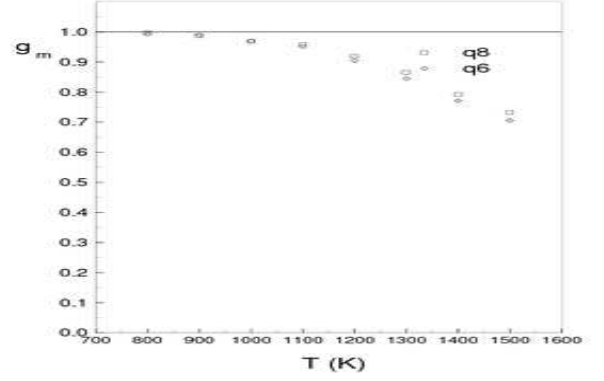


FIG. 16: g_m as a function of T .

B. Gaussian Approximation

In following Figs. 17, 18, 19, and 20 we have calculated the self-part intermediate scattering function $\Phi(q, t)$ by using Gaussian approximation, also according to Eqs.(17) and (18). As input data for both equations are the mean squared displacement (MSD) and the velocity autocorrelations functions obtained from our MD-Data. From figures we found that the gaussian approximation is correct in the short-time regime, here also for $t < 0.2$ ps. For $t > 0.2$ ps the course of $\Phi(q, t)$ resulting from this approximation deviates from both MD-results and MCT-analysis-results. As mentioned in Subsection III B we have assumed that the DOS of phonons is equally approximated to the spectral distribution of velocity autocorrelations function (VACF). With this assumption we can state now that the phonon-regime in our system is the regime taken place in a range time smaller then 0.2 ps. This time is a nearly temperature-independent time.

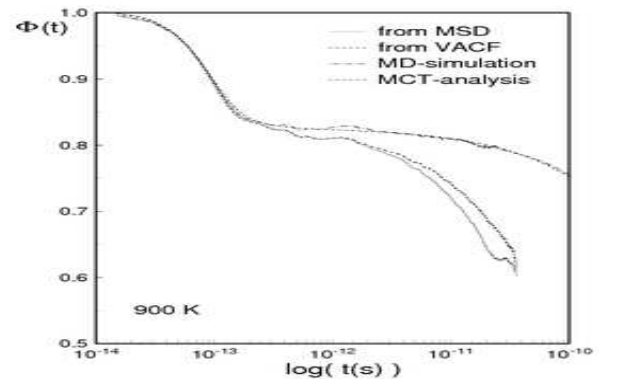
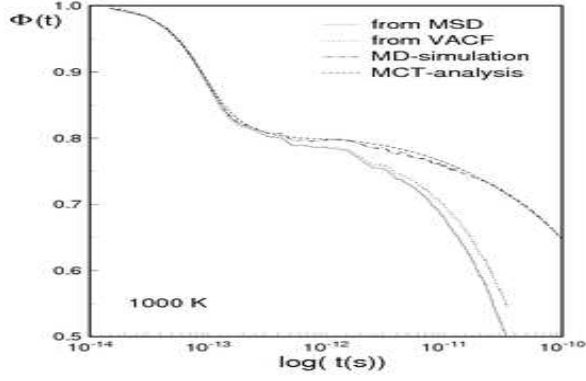
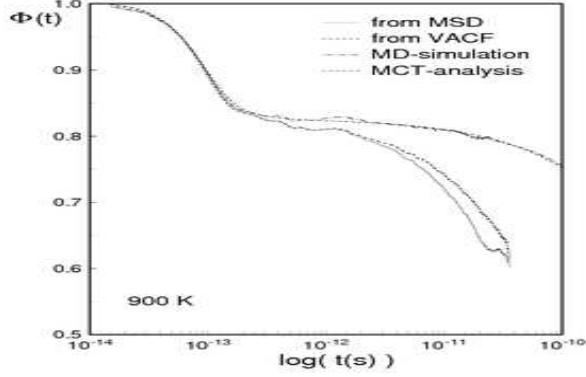


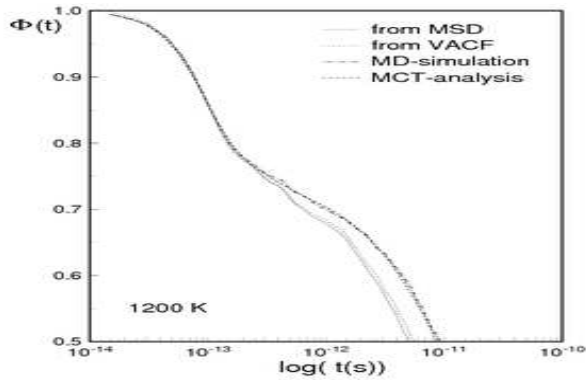
FIG. 17: The self-part of the intermediate scattering function for $T = 900$ K, according to Eqs. (17)(line) and (18)(dotted line), MD-result (dotted - dashed line), MCT-analysis (dashed line).

FIG. 18: The same as Fig.17 but for $T = 1000$ K.FIG. 19: The same as Fig.17 but for $T = 1100$ K.

To gain more our statement that this regime is as a result of the phonon vibrations we borrow a important relation of the liquid theory, namely, the relation between the spectral distribution of VACF and the susceptibility of the self-part intermediate scattering function $\Phi(q, t)$. According to theory that relation is approximated for a small q -value ($\lim q \rightarrow 0$) as follows [25, 26]

$$\chi''(\omega) = \omega \Phi_c(\omega) \approx q^2 Z(\omega) / \omega \quad (35)$$

Fig.21 presents our calculating results of Eq.(35) with

FIG. 20: The same as Fig.17 but for $T = 1200$ K.

an assumption that our q_8 -value is small enough. The calculating results show a fast nearly good agreement with that from the MCT-analysis (or a directly Fourier-transformed $\Phi(q, t)$).

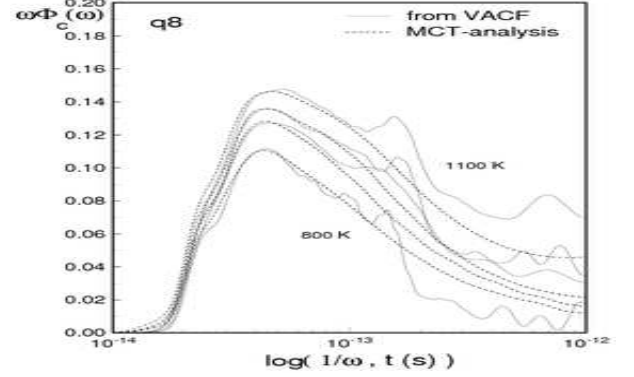


FIG. 21: The susceptibility obtained from the spectral distribution of VACF through Eq.(35) (lines) and from the MCT-analysis (dashed lines)

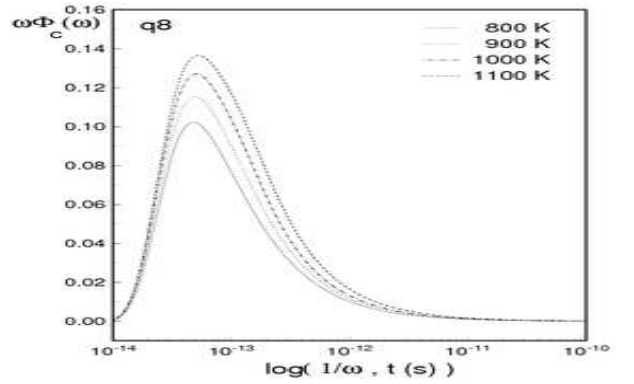
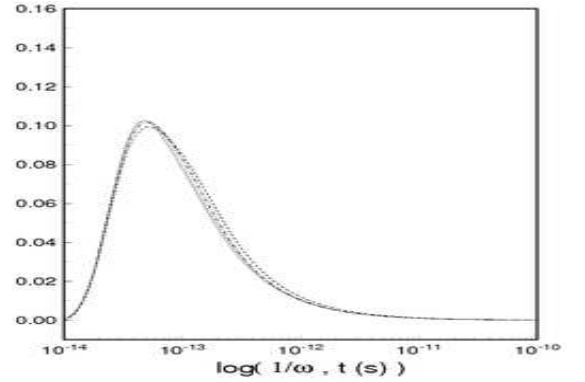
FIG. 22: The susceptibility obtained before superposition for wave vector q_8 .

FIG. 23: The susceptibility obtained after superposition.

Actually we can do a inverse Fourier-transformation of the susceptibility obtained from Eq.(35) to find back

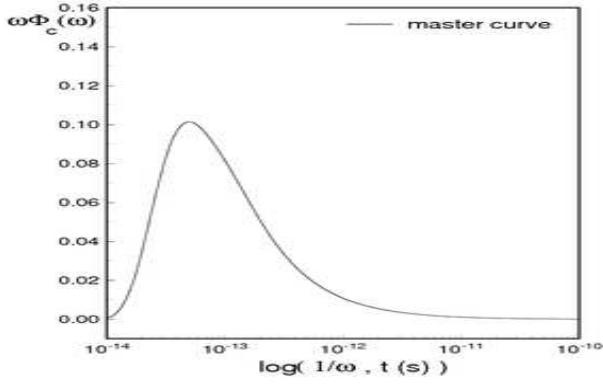


FIG. 24: The master curve of the susceptibility for q_8 according to Eq.(28).

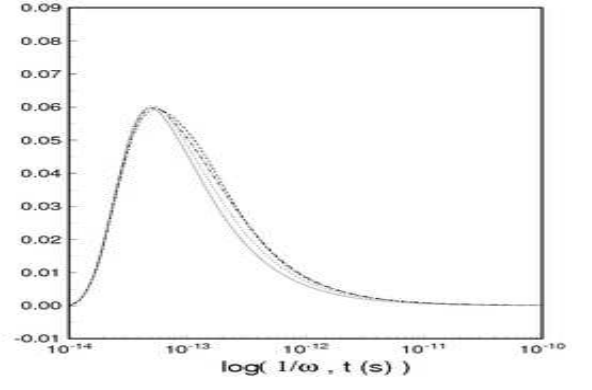


FIG. 27: The susceptibility obtained after superposition.

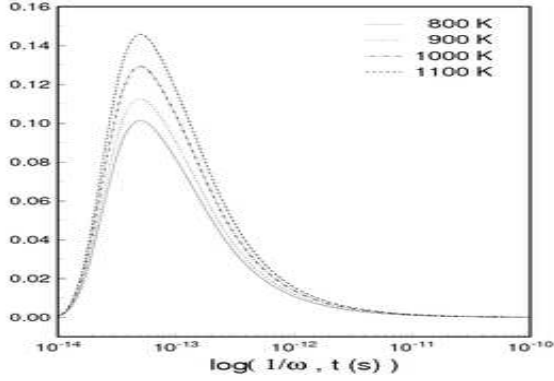


FIG. 25: The new susceptibility after scaling for q_8 according to Eq.(27).

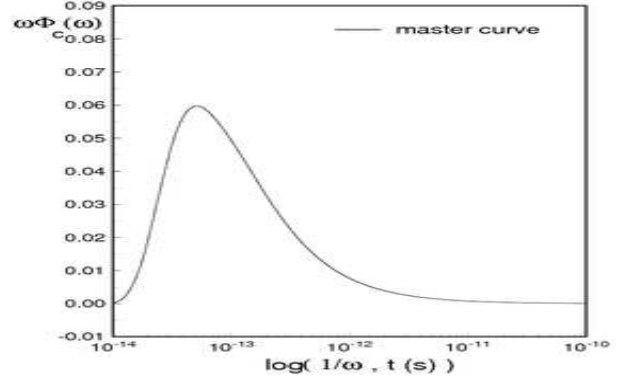


FIG. 28: The master curve of the susceptibility for q_6 according to Eq.(28).

the self-part intermediate scattering function $\Phi(q, t)$, but from the result shown in Fig.21 we do not do it, because Eq.(35) is a approximated relation that is really correct if the wave vector q is very small ($\lim q \rightarrow 0$ or, as one calls it, q is in a hydrodynamics limit), and then if we attempt to back Fourier transform of its susceptibility, surely we can not find a better $\Phi(q, t)$ as it found through Eq.(18).

Further discussion about susceptibility we attempt to separate the susceptibility of this phonon-regime from the full susceptibility. As mentioned in Sec. III we assume that this separation is really to find a purely susceptibility of this regime. Our result for two wave vector is shown in Figs. 22 and 26. We scale now these susceptibilities, the result is shown in Figs.23 and 27, here we have chosen as a arbitrary normalization of temperature, T_0 , 800 K, and

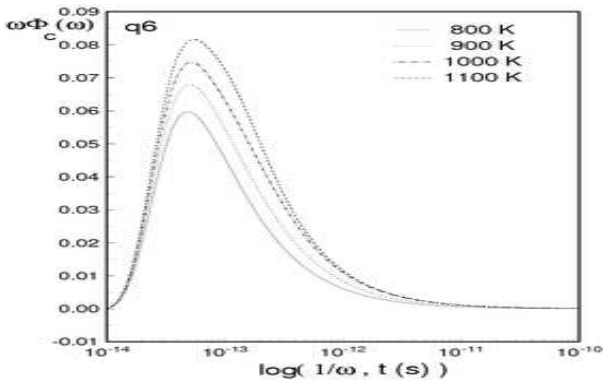


FIG. 26: The susceptibility obtained before superposition for wave vector q_6 .

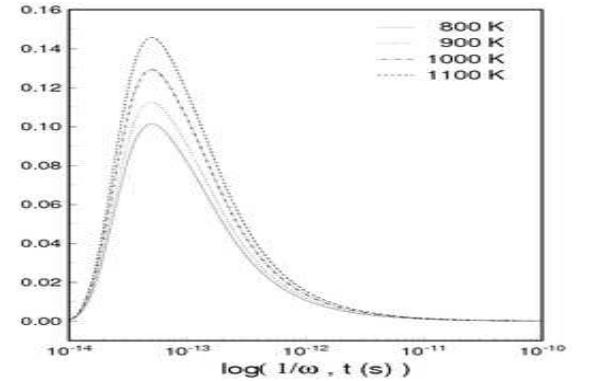


FIG. 29: The new susceptibility after scaling for q_6 according to Eq.(27).

we average these scaled susceptibilities through Eq.(3.14) to obtain the master curve of the susceptibility in this regime (see Figs.24 and 28). By using Eq.(27) we obtain the new susceptibility of this regime (see Figs. 25 and 29).

Adding the new susceptibility as shown in Figs.25 and 29 with the susceptibilities from other regimes, then we obtain the full susceptibility in the short-time regime as shown in Figs. 30 and 31. From both figures we found that the peaks of the new full susceptibility for temperatures 1000 K and 1100 K are higher than those old ones, but that peaks for temperatures 800 K and 900 K are lower than those old ones.

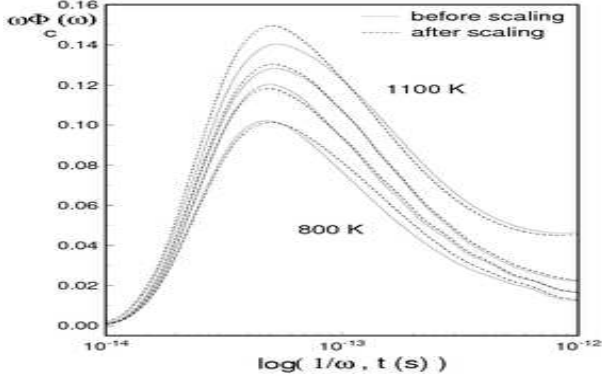


FIG. 30: The full susceptibility before (dashed lines) and after scaling (full lines) in a short-time regime for wave vector q_8 .

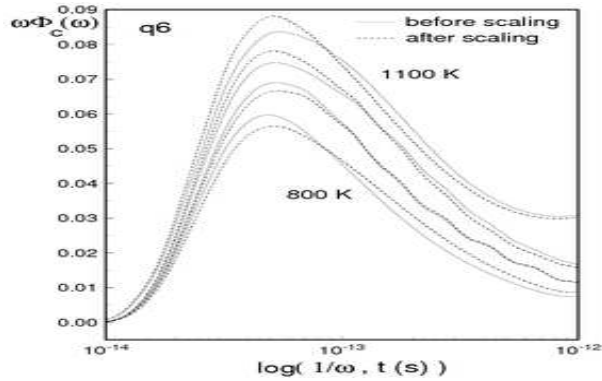


FIG. 31: The full susceptibility before (dashed lines) and after scaling (full lines) in a short-time regime for wave vector q_6 .

Taking back Fourier transformation of $\Phi_c(\omega)$ of the new full susceptibility in the short-time regime, then we obtain the new $\Phi(q, t)$ as shown in Figs. 32 and 33. The deviation of the new $\Phi(q, t)$ from the old one for each temperature of interest is taken place at a time range that is smaller than 0.5 ps.

It is interesting to calculate the new kernel $F(t)$ and the new $G(\Phi)$ -function in this short-time regime. Our results for the kernel $F(t)$ are shown in Figs. 34 and 35.

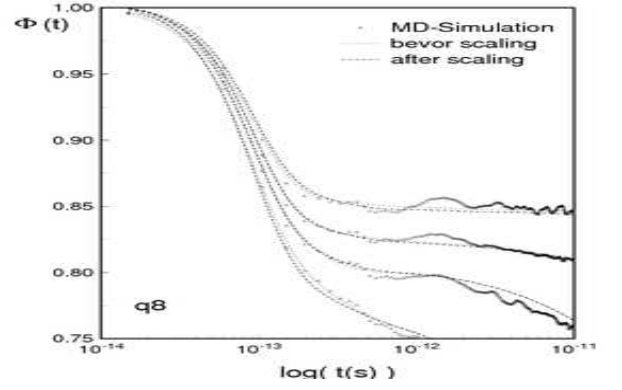


FIG. 32: The self-part of the intermediate scattering function in a short-time regime, MD-results (Symbol), before (dotted line) and after scaling (dashed-line) for wave vector q_8 .

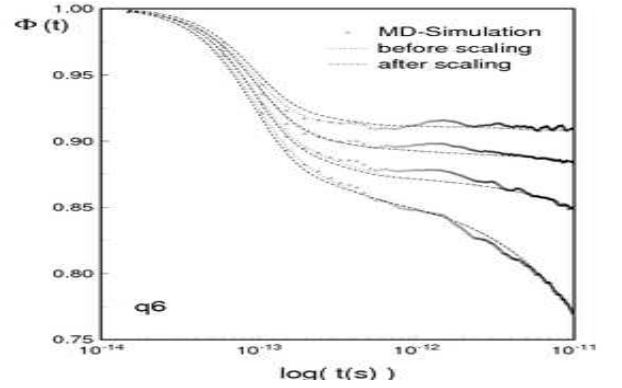


FIG. 33: The self-part of the intermediate scattering function in a short-time regime, MD-results (Symbol), before (dotted line) and after scaling (dashed-line) for wave vector q_6 .

The new kernel $F(t)$ for each temperatures of interest show more regular than the old one. The deviation of the new kernel from the old one is taken place at a time range that is smaller than 0.5 ps, also this time range is the same as it found in the case of $\Phi(q, t)$. It is clear that $\Phi(q, t)$ in this regime depends strongly on the kernel $F(t)$.

V. CONCLUDING REMARKS

Our system behaves as predicted by the schematic MCT-Modell, in the sense that the self-part intermediate scattering function $\Phi(q, t)$ shows at lower temperature three step of the structural relaxation. The behavior of the self-part intermediate scattering function $\Phi(q, t)$ agrees well for the long time with the prediction of the extended schematic MCT-Model in the sense that the self-part intermediate scattering function $\Phi(q, t)$ always decays to zero after long times as a result of thermally activated atomic diffusion.

The behavior of the memory kernel $F(t)$ agrees with the prediction of the extended MCT-Model in the sense

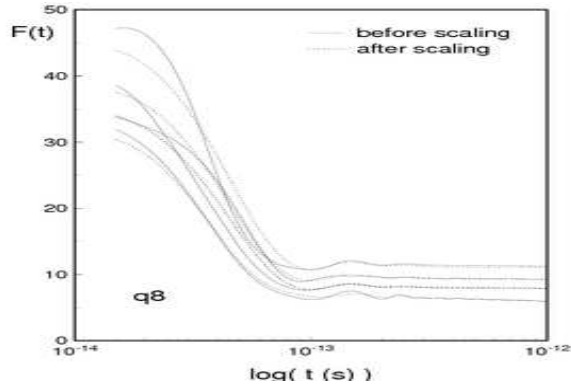


FIG. 34: The kernel $F(t)$ in the short-time regime before (full lines) and after scaling (dotted lines) for wave vector q_8 .

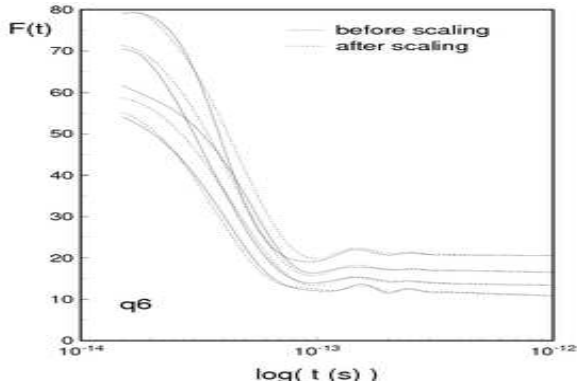


FIG. 35: The kernel $F(t)$ in the short-time regime before (full lines) and after scaling (dotted lines) for wave vector q_6 .

that the behavior of $F(t)$ below $\Phi_0(t)$ corresponds to a polynomial function that has non-negative coefficients. This behavior depends strongly on the wave vector q .

As in I, to determine approximately the critical temperature T_c we have used the maximum g_m of the characteristic function $g(\Phi)$. We obtain $T_c \approx (1025 \pm 25)$ K for our system.

Through the temperature superposition method in a short times regimes our results show that the vibration-phonon regime is really as a result of the harmonic phonon approximation, and then this regime can be good described by a gaussian approximation. In the case of a gaussian approximation, which follows from the liquid state theory, the courses of the self-part intermediate scattering function $\Phi(q, t)$ resulted from both VACF and MSD shows at time, $t \approx 0.5$ ps a deviation from the proper courses obtained from MD-simulations and MCT-analysis

Acknowledgments

A.B.M. gratefully acknowledges financial support of the DAAD during the post-doctoral program.

-
- [1] H.Z. Cummins, G. Li, Y.H. Hwang, G.Q. Shen, W.M. Du, J. Hernandez, and N.J. Tao, *Z.Phys. B* **103**, 501 (1997).
 - [2] L.P. Kadanoff and J. Swift, *Phys. Rev.* **166**, 89 (1968).
 - [3] K. Kawasaki, *Phys. Rev.* **150**, 1 (1966); *Ann. Phys. (N.Y.)* **61**, 1 (1970).
 - [4] M.H. Ernst and J.R. Dorfman, *J. Stat. Phys.* **12**, 311 (1975).
 - [5] U. Bengtzelius, W. Götze, and A. Sjölander, *J. Phys. C* **17**, 5915 (1984).
 - [6] E. Leutheusser, *Phys. Rev. A* **29**, 2765 (1984).
 - [7] P.S. Das and G.F. Mazenko, *Phys. Rev. A* **34**, 2265 (1986).
 - [8] W. Götze and L. Sjörgen, *J. Phys. C* **21**, 3407 (1988).
 - [9] L. Sjörgen, *Z. Phys. B* **79**, 5 (1990).
 - [10] H. Teichler, *Phys. Rev. E* **53**, 4287 (1996).
 - [11] F. Mezei, W. Knaak, and B. Farago, *Phys. Rev. Lett.* **58**, 571 (1987); W. Knaak, F. Mezei, and B. Farago, *Europhys. Lett.* **7**, 529 (1988).
 - [12] M. Kiebel, E. Bartsch, O. Debus, F. Fujara, and H. Sillescu, *Phys. Rev. E* **45**, 10301 (1992).
 - [13] A. Fontana, F. Rocca, M.P. Fontana, B. Rosi, and A.J. Dianoux, *Phys. Rev. B* **41**, 3778 (1990).
 - [14] H.Z. Cummins, G. Li, M. Du, and A. Sakai, *Phys. Rev. A* **46**, 3343 (1992).
 - [15] W. van Meegen and S.M. Underwood, *Phys. Rev. E* **49**, 4206 (1994).
 - [16] W. Kob and H.C. Andersen, *Phys. Rev. E* **51**, 4626 (1995); *ibid.* **52**, 4143 (1995).
 - [17] L.J. Lewis and G. Wahnström, *Phys. Rev. E* **50**, 3865 (1994); L.J. Lewis, *Phys. Rev. B* **44**, 4245 (1991).
 - [18] H. Teichler, *Phys. Rev. Lett.* **76**, 62 (1996).
 - [19] Ch. Hausleitner and Hafner, *Phys. Rev. B* **45**, 128 (1992).
 - [20] H. Teichler, *Phys. Status Solidi B* **172**, 325 (1992).
 - [21] A.B. Mutiara, Diplomarbeit, Göttingen (1996).
 - [22] W. Götze, *Z. Phys. B* **60**, 195 (1985).
 - [23] G. Buchalla, U. Dersch, W. Götze and L. Sjörgen, *J. Phys. C* **23**, 4239 (1988).
 - [24] W. Götze and R. Haussmann, *Z. Phys. B* **72**, 403 (1988).
 - [25] B.J. Boon and S. Yip, *Molecular Hydrodynamics*, (McGraw-Hill, 1980).
 - [26] J.-P. Hansen and I.R. McDonald, *Theory of Simple Liquids*, 2nd Ed. (Academic Press, London, 1986).
 - [27] U. Balucani and M. Zoppi, *Dynamics of the Liquid State*, (Clarendon Press, Oxford, 1994).
 - [28] B.R.A. Nijboer and A. Rahman, *Physica (Utrecht)* **32**,

- 415 (1966).
- [29] C.M. Roland and K.L. Ngai, J. Chem. Phys. **103**, 1152 (1995).
 - [30] R. Zorn, A. Arbe, J. Colmenero, B. Frick, D. Richter, and U. Buchenau, Phys. Rev. E **52**, 781 (1995).
 - [31] S.W. Lovesey, *Theory of Neutron Scattering from Condensed Matter*, Vol.1 (Clarendon Press, Oxford, 1987).
 - [32] A.P. Sokolov, E. Rössler, A. Kisliuk, and D. Quitmann, Phys. Rev. Lett. **73**, 2062 (1993); E. Rössler, A.P. Sokolov, A. Kisliuk, and D. Quitmann, Phys. Rev. B **49**, 14967 (1994).
 - [33] A.K. Hasan, L. Börjesson, and L.M. Torell, J. Non-Cryst. Solids **172-174**, 154 (1994).
 - [34] J. Habasaki, I. Okada, and Y. Hiwatari, Phys. Rev. E **52**, 2681 (1995).
 - [35] T. Muranaka and Y. Hiwatari, Phys. Rev. E **51**, 2735 (1995).
 - [36] C.A. Angel, J. Non-Cryst. Solids **73**, 1 (1985).
 - [37] G. Wahnström, Phys. Rev. A **44**, 3752 (1991).
 - [38] G.F. Signorini, J.-L. Barrat, and M.L. Klein, J. Chem. Phys. **92**, 1294 (1990).
 - [39] H. Löwen, J.-P. Hansen, and J.-N. Roux, Phys. Rev. A **44**, 1169 (1991).
 - [40] H. Teichler, in: *Simulationstechniken in der Materialwissenschaft*, edited by P. Klimanek and W. Pantleon (TU Bergakademie, Freiberg, 1996).
 - [41] T. Aspelmeier, Diplomarbeit, Göttingen (1995).
 - [42] J.-P. Hansen and S. Yip, Transp. Theory Stat. Phys. **24**, 1149 (1995).
 - [43] B. Bernu, J.-P. Hansen, G. Pastore, and Y. Hiwatari, Phys. Rev. A **36**, 4891 (1987); *ibid.* **38**, 454 (1988).
 - [44] W. Götze and L. Sjörgen, Rep. Prog. Phys. **55**, 241 (1992).
 - [45] J. Colmenero, A. Arbe, A. Alegria, and K.L. Ngai, J. Non-Cryst. Solids **172-174**, 229 (1994).
 - [46] H. Teichler (unpublished).
 - [47] J.-N. Roux, J.-L. Barrat, and J.-P. Hansen, J. Phys. Cond. Matt. **1**, 7171 (1989).